Inclus
Methc

Daniel Sa

THE SO-
mance of p
Marine Te
This me
to this dat
tal hydroc
faces (lift,
termine t
wetted ke
ing tender
loading, d
dynamic e
area aft of
tom area f
spray are
contributi
oped or v
speeds of p
that the w
be ignored
In 1964
model test
the bottom
whisker s
that by th
speed resi
clearly de

[1] Profess
[2] Researc
[3] Researc
stitute of T
Presente
Society of N
Manuscr

bottom. T
the spray
stagnatio
computed
total weti

The otl
tion line
surface E
photogra]
by other
this time
analytica
hull.

The di
that the
velocity a
between
tion line;
a reflecti
stream ve
Fig. 4, ta
striations
the botto
striations
area). By
of the inc

Since t
then usi
taken to
water ph
er spray
undisturl
edge of tl

As thi
sembles
model sc
in full sc
This is d
forces are
spray an

Ap =

As =

Aas =

b =

b_{sr} =
C =
Cf =
Fs =

F_{∇} =

g =

L =
Lc =

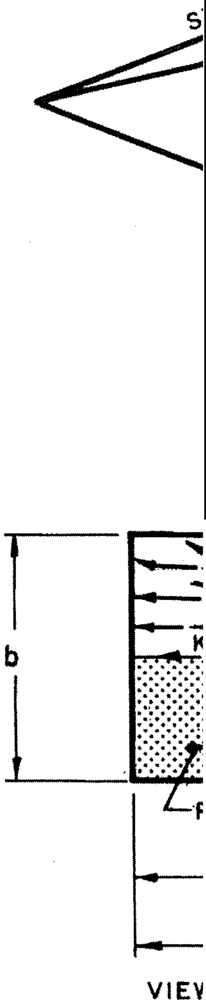

Angle between stagnation l

Edge of whisker spray

Angle between the keel and

Whisker spray area; As = a

s

Also, but not shown on this

Deadrise angle = β

Equilibrium trim angle = τ

Each of these quantities is ol

***Lk* and *Lc*.** For a given loac and speed, application of t method for planing hulls giv vide the equilibrium trim a values of Lk and Lc.

Angle α. Savitsky (1964) d which identifies the angle, α, angle and deadrise angle:

Fi

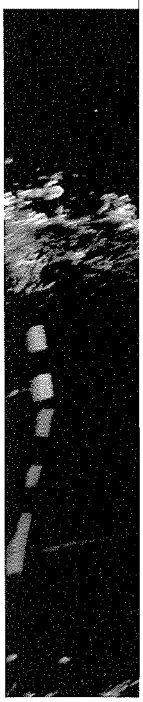

Fig. 3 Charact

Using the above definit
be shown that the total
hull) projected on the pl
lar to the hull centerpl

As

Using the previous defi

tan

Substituting into equat

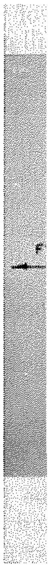

the whi
line. In
as a refe
ing the
only slig
effect o
identifie
of the pr
tifies its
Equat
that the
Referrin

Then, fo
relative
above, t
tion so t
case the
fact that
gravity
induced
reduce t
Weinste
planing
Quoting
tan τ) ex
tive frict
spray is
respect t
region o
that the
opposite
thereby
p. 6).
The p
tions of
the spra
than 90
directed
resistan
The rela
of trim

In order to simplify this equation for easy application by the practicing naval architect, let:

$$Rs = \Delta\lambda\, b^2 \frac{1}{2} \rho V^2 Cf = \frac{1}{2} \rho V^2 \frac{b^2 \cos \Theta}{4 \sin 2\alpha \cos \beta} Cf \qquad (11)$$

The quantity $\Delta\lambda \times b^2$ represents the increase in effective wetted bottom surface area that is attributed to the whisker spray contribution to total resistance.

Solving for the quantity $\Delta\lambda$,

$$\Delta\lambda = \frac{\cos \Theta}{4 \sin 2\alpha \cos \beta} \qquad (12)$$

This expression is plotted in Fig. 5, where the dependence of $\Delta\lambda$ on trim and deadrise is most obvious. It is seen that for combinations of small trim angles and high deadrise angles, which are typical for high-speed planing hulls, the added spray resistance will be maximum. Thus, the contribution of the spray viscous force to the total hull resistance can then be written as:

$$Rs = \frac{1}{2} \rho V^2 \Delta\lambda\, b^2 Cf \qquad (13)$$

where

$\Delta\lambda$ is obtained from Fig. 5
b = beam of the planing hull (feet)
V = planing velocity (feet/second)
Cf = discussed below.

It will be noted from Fig. 5 that for specific combinations of τ and β, the quantity $\Delta\lambda$ is equal to zero. While there will be a noticeable whisker spray breaking away from the chines at these conditions, the direction of its velocity is normal to the keel. Hence, there is no longitudinal component of the viscous force and consequently no drag component so that $\Delta\lambda = 0$.

Figure 6 is a graphical illustration o
angle on whisker spray drag for a 15 deg
ating at a mean wetted length beam ratio
spray area (shaded area), the total viscou
area (Fs), and the resistance component (
for trim angles of 2 deg, 4 deg, and 9.5 de
the lowest trim angle, 2 deg, the whisker
its aft orientation are substantially large
trim angles. In this example the largest v
2 deg trim. As the trim angle is increas
are reduced, and finally at a trim angle
rected normal to the keel so that its resis
zero. At that point $\Delta\lambda$ is also zero, as sh

For combinations of small trim angles
angles (which are typical for very high-s
$\Delta\lambda$ is relatively large so that the spray
will be significant. As will be shown
whisker spray drag can be as large as 15
Fortunately, short longitudinal spray
ciously attached to the bottom to deflect
avoid the large increase in drag. This re
ance as to the proper location, size, an
spray strips as a function of hull geor
speed.

3.3. Estimate of friction coefficient (

In this study the density and viscosit
whisker spray area are taken to be tha
fluid at the ambient temperature and sal
shape of the spray area is triangular (Fi
istic length of the whisker spray (Lws) is
length of the forward edge of the spray t
the bottom. The velocity of the spray she
velocity, V. Thus, the Reynolds numbe
spray sheet is:

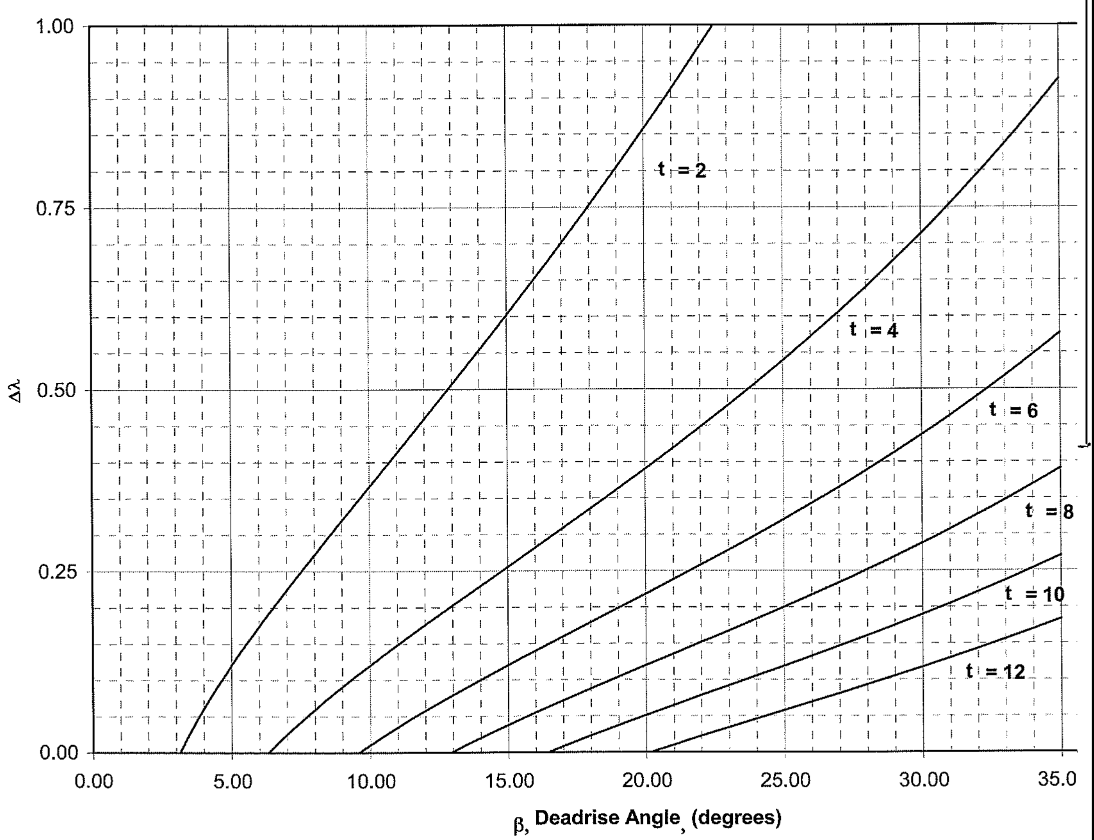

Fig. 5 Incremental increase in $\Delta\lambda$ due to spray contribution to drag

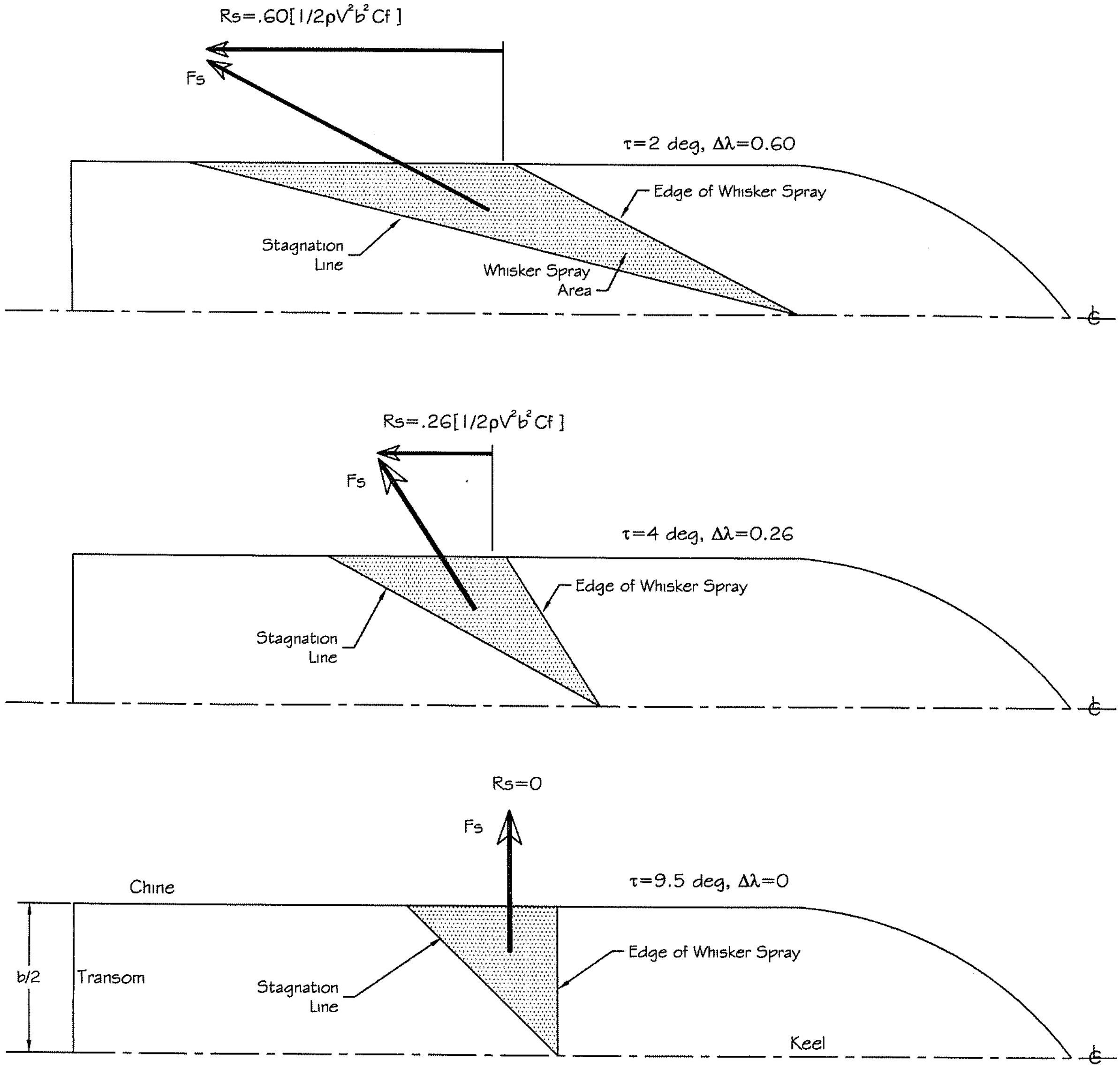

Fig. 6 Reduction of whisker spray resistance (*Rs*) with increasing trim angle, β = 15 deg, λ = 1.5

$$RNws = \frac{V\,Lws}{\nu} \tag{14}$$

Using the geometric relations previously identified, the value of *Lws* is:

$$Lws = \frac{1}{2} \times \frac{b/2}{\sin 2\alpha \cos \beta} \tag{15}$$

Note that *Lws* will be substantially smaller than the mean wetted length of the pressure area defined as $(Lk + Lc)/2$. Hence, the Reynolds number in the spray area will also be much smaller than that of the pressure area. Further, it has been shown by Savitsky and Breslin (1958) that the fluid in the spray sheet consists of a thin layer of the oncoming free-surface fluid, which is reflected from the stagnation line. It is expected that the level of free turbulence in this layer of fluid is quite small. These observations raise some question as to the state of the model boundary layer in the whisker spray area.

In 1952, Savitsky and Ross conducted a series of model tests using a 5 in. beam, 20 deg deadrise planing hull to determine the state of the boundary layer over a range of Reynolds numbers. A chemical paint detection technique (described in Savitsky & Ross 1952) was used to define the flow patterns over the bottom. The paint was white and was sprayed on the hull bottom, which was painted black. Its special characteristic was that it would dissolve from the bottom in turbulent areas, thus exposing the black base color of the model. It would remain white on the bottom where the flow was laminar. In these tests, the model was removed from the towing apparatus after each run and the hull bottom was photographed to record the laminar (white) and turbulent flow (black) areas.

It was found that the flow in the whisker spray area was laminar or in a state of transition from laminar to turbulent flow. Figure 4 shows that nearly the entire whisker spray area was laminar (white color) for the test condition of 6 deg trim and a speed of 13.02 feet/second. Using the above equations, the average Reynolds number of that spray sheet was $RNws = 1.5 \times 10^5$. This relatively small Reynolds number plus the expected low ambient turbulence level implies an extensive area of laminar flow, thus confirming the experimental observation.

At larger Reynolds numbers it is expected that some portions of the spray area will become turbulent resulting in a combination of laminar and turbulent flow. According to

Schlichting (1960, p. 538), the boundary layer will be laminar to begin with and will change to a turbulent one further downstream. The position of the point of transition will depend on the intensity of turbulence in the external flow field and will be defined by the value of the critical Reynolds number, RN_{crit}, which ranges between 3×10^5 and 3×10^6. The viscous drag coefficient, *Cf*, including the effects of mixed laminar and turbulent flow, is identified by Schlichting as:

$$Cf = \frac{0.074}{\sqrt[5]{RN}} - \frac{A}{RN} \tag{16}$$

where the constant *A* is related to the Reynolds number at the position of initial transition from laminar to a mixed laminar and turbulent flow. It is called the critical Reynolds number = RN_{crit}. This equation is the Prandtl-Schlichting skin friction formula for a smooth flat plate at zero incidence (Schlichting 1960).

The transition point is determined from experimental observations. It is dependent on the intensity of the turbulence in the external flow. A typical curve of *Cf* versus RN_{crit} in the transition range is shown as curve (3a) in Fig. 7 for an assumed transitional $RN_{crit} = 5 \times 10^5$ (Schoenerr 1932). In this case $A = 1{,}700$. It is seen that as *RN* exceeds RN_{crit}, *Cf* initially increases from its laminar flow value of 0.00188, attains a maximum value, and then decreases for further increases in *RN* and follows the fully turbulent friction curve at large *RN*.

In the present study the value of *A* was estimated by using data from Clement (1964a, 1964b), where the resistance of the whisker spray was inferred by comparing model test data with and without spray deflectors installed on the hull bottom. Converting the whisker spray drag to a friction coefficient, and knowing its Reynolds number, allowed for a determination of the value of *A* in equation (16). The value of *A* was found to be approximately 4,800. This corresponds to a whisker spray $RN_{crit} = 1.5 \times 10^6$ that is well within the range of critical Reynolds numbers specified by Schlichting.

For $RNws < 1.5 \times 10^6$, the flow is assumed to be laminar and the viscous friction coefficient is taken to be the Blasius formulation (Schlichting 1960).

$$Cf(\text{laminar}) = \frac{1.328}{\sqrt{RNws}} \tag{17}$$

The importance of this discussion of the transition of the boundary layer from laminar to turbulent flow pertains mainly to model test results where, for commonly used model sizes, the *RNws* will be small enough so that the whisker spray boundary layer will either be fully laminar or in some transitional state between a fully laminar and a fully turbulent state. It may be noted that artificial means for stimulation of turbulence in planing hull model tests are rarely used.

The full-scale craft will operate at much higher RN_{ws}, where it is expected that the whisker spray boundary layer will be fully turbulent. In this case, the turbulent friction coefficients such as defined by the Schoenherr friction line (also referred to as the ATTC line) may be used (SNAME 1948). In summary, the following formulations for estimating the viscous friction coefficient of the whisker spray measured in model tests of Clement (1964a, 1964b) are expected to apply:

For $RNws < 1.5 \times 10^6$ (laminar flow):

$$Cf = \frac{1.328}{\sqrt{RNws}} \tag{18}$$

For $RNws \geq 1.5 \times 10^6$ (transitional flow):

$$Cf = \frac{0.074}{\sqrt[5]{RNws}} - \frac{4{,}800}{RNws} \tag{19}$$

This equation is plotted in Fig. 7, curve (5). As expected, because of the larger value of RN_{crit}, the values of *Cf* are less than those given by the transition curve (3a), and the transition to fully turbulent flow occurs at relatively larger *RN*. This implies a more stable boundary layer in the model bottom area wetted by the fluid that comprises the whisker spray. Because this equation is based on a limited number of available model data, there is still some concern about its applicability to the relatively thin layer of fluid that flows along the hull bottom. Further analytical and experimental studies of the viscous characteristics of this relatively thin

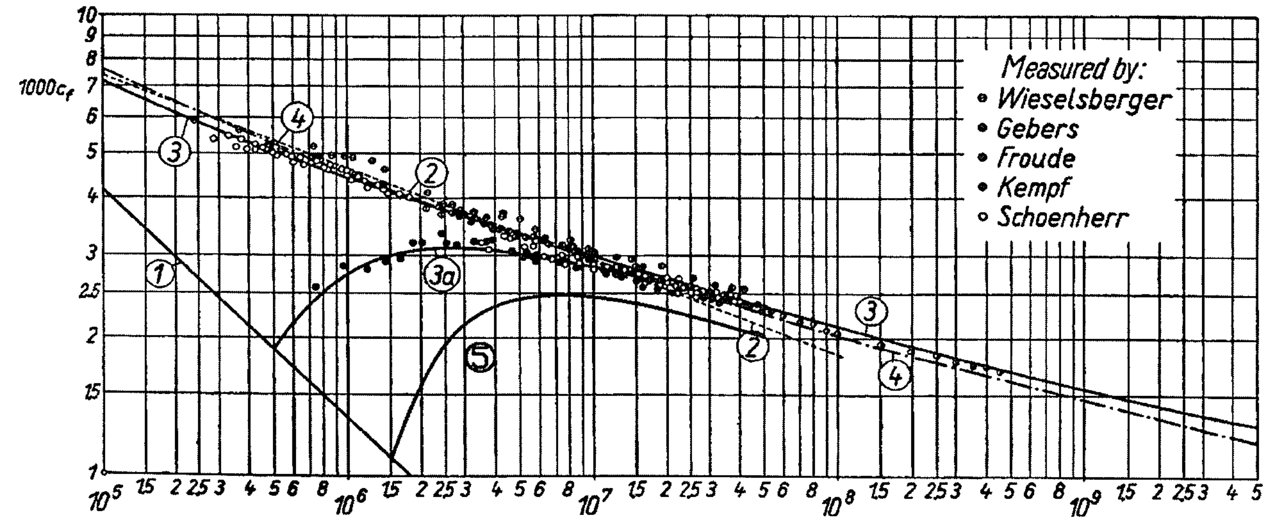

$$RN = \frac{U_\infty l}{\nu}$$

$$\text{Curve (1): Laminar Flow: } Cf = \frac{1.328}{\sqrt{RN}} \qquad \text{Curve (5): Transitional Flow: } Cf = \frac{0.074}{\sqrt[5]{RN}} - \frac{4800}{RN}$$

Fig. 7 Classical resistance formula for smooth flat plate at zero incidence; comparison between theory and measurement (Schoenerr 1932) layer of flow are strongly recommended. Of particular usefulness would be experiments that directly measure the whisker spray drag and relate these results to model size. Of course, full-scale tests would be invaluable.

In conclusion, transitional flow equations, such as in equations (18) and (19), should be applied to model test results where the boundary layer is expected to be in a laminar or transitional state. Because the value of A in equation (16) is governed by the environmental conditions in a test facility, the transitional flow equation may be different in different towing tanks. For full-scale predictions, where the boundary layer is expected to be fully turbulent, the Schoenherr or ITTC lines should be used. In this case the pressure area and the spray area will have different Reynolds numbers and hence different viscous drag coefficients.

4. Validation of whisker spray drag equation

Wherever possible, the results of analytical predictions should be verified by comparison with experimental results. Unfortunately, there are no direct measurements of the whisker spray drag in the published literature. However, there are three sources of model test data that can be used indirectly to obtain estimates of spray drag that can be compared with the recommended equation for spray drag. These are:

1. A series of model test results that demonstrated the effectiveness of judiciously located bottom spray strips in reducing the total resistance of high-speed planing hulls (Clement 1964a, 1964b). The whisker spray drag was inferred from the test data and then compared with the computed drag.
2. A series of high-speed model tests performed by Kapryan and Boyd (1953) on a 20 deg deadrise prismatic hull over a wide range of trim angles and wetted lengths. By comparing the total model friction drag coefficient with the Schoenherr turbulent friction line, it was possible to identify the whisker spray drag.
3. Model test results of a number of arbitrarily selected planing hulls where the measured total resistance is compared with the computed total resistance that includes hull resistance + whisker spray resistance + aerodynamic resistance. These results provide for a validation of the performance prediction method as originally presented in Savitsky (1964) but now expanded to include the spray drag and bare hull aerodynamic resistance as measured in model tests. For full-scale craft, the aerodynamic drag of the superstructure must of course also be included.

Prior to discussing these model tests, it is important to note that, in most test reports the model data have been extrapolated to and are presented as full-scale values. This raises the question as to how the model whisker spray resistance has been extrapolated to the larger Reynolds numbers of the full-scale craft. The answer is that at the present time no separate extrapolation is made of the whisker spray resistance to account for their Reynolds numbers in the full-scale craft. The current procedure is to use only the wetted bottom area aft of the stagnation line in calculating the model viscous resistance and then subtract this from the total measured resistance (which is the sum of induced pressure drag + viscous drag in the bottom area aft of the spray root line + the whisker spray drag + aerodynamic drag) to obtain the residual drag. The part of the bottom area that is wetted by the whisker spray is customarily neglected (Clement & Blount 1963). Consequently, the model viscous spray drag component is, by default, contained in the calculated model residual drag and is therefore Froude scaled.

Since the full-scale residual drag is taken to be equal to the model residual drag multiplied by the cube of the scale ratio, it consequently scales the model whisker spray drag by the cube of the scale ratio. This implies that the friction coefficient in the spray area is the same for the model and full scale, which of course is not correct. The published data are nevertheless quite useful since they can be used to isolate the resistance of the model whisker spray drag, for which the Reynolds number is known, and then to compare these experimental results with analytical predictions using the Cf versus RN relations given by equations (18) and (19). This procedure is applied in the following sections of this report.

Each of the above validation efforts is discussed in the following sections.

4.1. Model tests with and without spray deflectors

In 1964, Clement (1964a, 1964b) conducted model tests on two planing hulls to examine the effectiveness of adding bottom spray strips to deflect the whisker spray away from the hull and thus reduce the total hydrodynamic resistance. Each model was tested with and without spray strips, and the results were presented as full-scale values. The difference in measured total resistance was used to identify the effectiveness of these strips and also, indirectly, to quantify the magnitude of the resistance of the whisker spray to the extent that it was deflected from the bottom.

A brief description is given of the model geometries, model scale, loading, size and location of spray strips, test results, and comparison between calculated and measured value of the whisker spray drag.

4.1.1. Results from Clement (1964a). The model used for these tests represented a 68 ft planing boat to a scale of 1/6. The model resistance data were converted to a full-scale displacement of 99,500 pounds using the Schoenherr coefficients of frictional resistance (also called the ATTC friction line) with zero roughness allowance. The body plan for this hull and the arrangement of the short spray deflector strips are shown in Fig. 8. The deadrise angle is 20.5 deg, and the equivalent full-scale beam measured between the chines is 15.6 ft (model beam = 2.6 ft). The bare hull (no bottom spray strips) performance results for this hull are given by the solid curves shown in Fig. 9. All results are presented in nondimensional form.

Longitudinal spray strips were then attached to the hull bottom, as shown in Fig. 8. As can be seen, they were relatively short and extended from just aft of the spray root line forward into the whisker spray area. Each strip deflects a portion of the whisker spray from the bottom and produces a local dry bottom area that extends from the outboard edge of the spray strip to the chine. By judiciously locating a number of such small spray strips (in a chevron-like pattern), as shown in Fig. 8, it is possible to deflect a substantial area of the whisker spray away from the bottom. The results of model tests with these spray strips are shown by the round symbols in Fig. 9. It is clear that the addition of spray strips reduced the high-speed resistance by 6% without an increase in low-speed resistance or changes in trim and heave.

The difference between the resistance of the bare hull and the hull with spray strips can be taken to be indicative of the whisker spray resistance. Since the plotted data also define the running trim angle versus speed, the spray drag was calculated for each speed using equation (13) of this report. The details of this calculation and results are tabulated below:

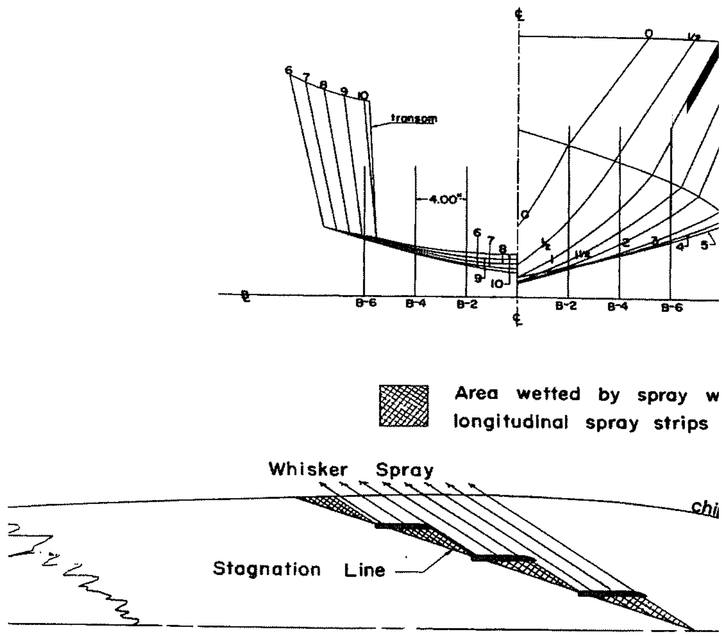

Fig. 8 Hull body plan and short spray strips used in model test

$$Rs = \frac{1}{2}\,\rho\, V^2\, \Delta\lambda\, b^2\, Cf$$

where

$\Delta\lambda = f(\tau,\beta)$ given in Fig. 5

b = beam of the planing hull model = 2.6 ft

V = model planing velocity (feet/second)

$$Cf = \frac{0.074}{\sqrt[5]{RNws}} - \frac{4{,}800}{RNws} \text{ (for transitional flow, } RNws \geq 1.5 \times 10^6\text{)}$$

$$Cf = \frac{1.328}{\sqrt{RNws}} \text{ (for laminar flow, } RNws < 1.5 \times 10^6\text{)}$$

$$RNws \text{ (model)} = \frac{V\, Lws}{\nu}$$

$$Lws = \frac{1}{2} \times \frac{b/2}{\sin 2\alpha \cos\beta}$$

The spray area used in this equation is the total wetted spray area as given by equation (7). However, Fig. 8 shows that the spray strips deflected only approximately 88% of the total spray area so that the Rs was taken to be 88% of the calculated value based on total spray area. Table 1 shows calculated values for the deadrise angle of 20.5 deg., and a displacement of Δ = 99,500 pounds.

These calculated values of spray-drag/displacement ratio were then subtracted from the bare hull drag/displacement ratios in Fig. 9 to obtain the hull resistance/displacement ratio when spray strips are added to the bottom. The results are plotted in Fig. 9 and show rather good agreement with the experimental results, thus providing some credibility to the proposed analytical method for estimating the drag of the whisker spray.

4.1.2. Results from Clement (1964b). Of course, the conclusions from a single test may be fortuitous. Fortunately, Clement conducted similar tests on a 1/10 scale model of hull No. 4666 of the Series 62 family of hard chine planing hulls

(Clement 1964l
spray deflector
length strips s
(1964b) and lon
root line and w
deadrise angle
measured betw
beam = 1.87 ft
a weight of Δ =
hull with and
ducted at a con
Clement (1964
these tests. Th
using the proc
ing that 88% of
ted (Table 2).

These calcul
were then sub
ratios in Fig.
ratio when spr
are also plotted
ment with the
at the highest
approximately
addition to th
highest speed

4.2. Model te

In 1953, Kap
an extensive se
in. beam, prism
that resulted i
these tests mea
ted length, cen
trim angles an
a wind screen
very small. Of
their analysis
culate the frict
drag coefficien
sured drag coe
model were ne

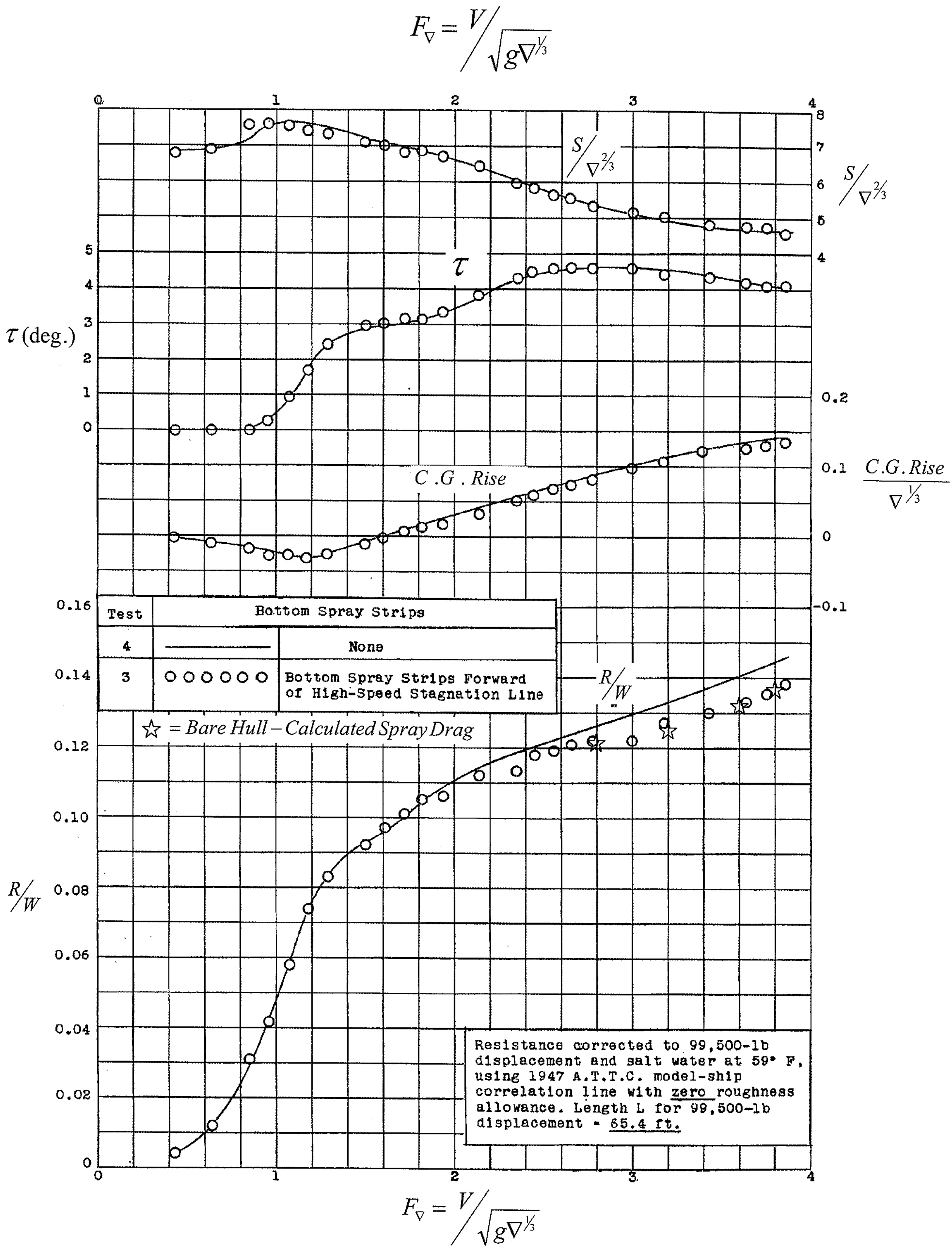

Fig. 9 Performance with no bottom strips and with short spray strips (from Clement 1964a) and comparison with spray drag calculated in present study

cous drag coefficient that includes the viscous forces on the bottom pressure area and the whisker spray area but normalized by only the bottom pressure area. The results are plotted against the hull Reynolds number on their Fig. 15 for the 20 deg deadrise hull along with the Schoenherr (ATTC) turbulent friction line. This plot is reproduced in the present report as Fig. 13. Although the drag data are somewhat scattered, the following trends can nevertheless be observed.

Table 1

$F\nabla$	τ (deg
2.8	4.7
3.2	4.5
3.6	4.2
3.8	4.0

* = ful
† = mo

Of par
cients ge
the mod
differenc
with inc
differenc
these dif
is appar
requires
of large-
The pr
calculate
the whis
cous for
that the
must be
pressure
for norm
larger fr
The fa
Schoenh
trim ang
teristics
5, the va
is larges
of 16 deg
consister
To qua
calculat
angles o
develope
culations
formula
coefficie
formulat
tests co
Taylor M
drag in
pressure
that the
that mo
perimen
Thus,
(1953) p
ing the r
this pap

4.3. Mo

4.3.1. C
methods
dynamic
with th
Savitsky
predictin
rudders,

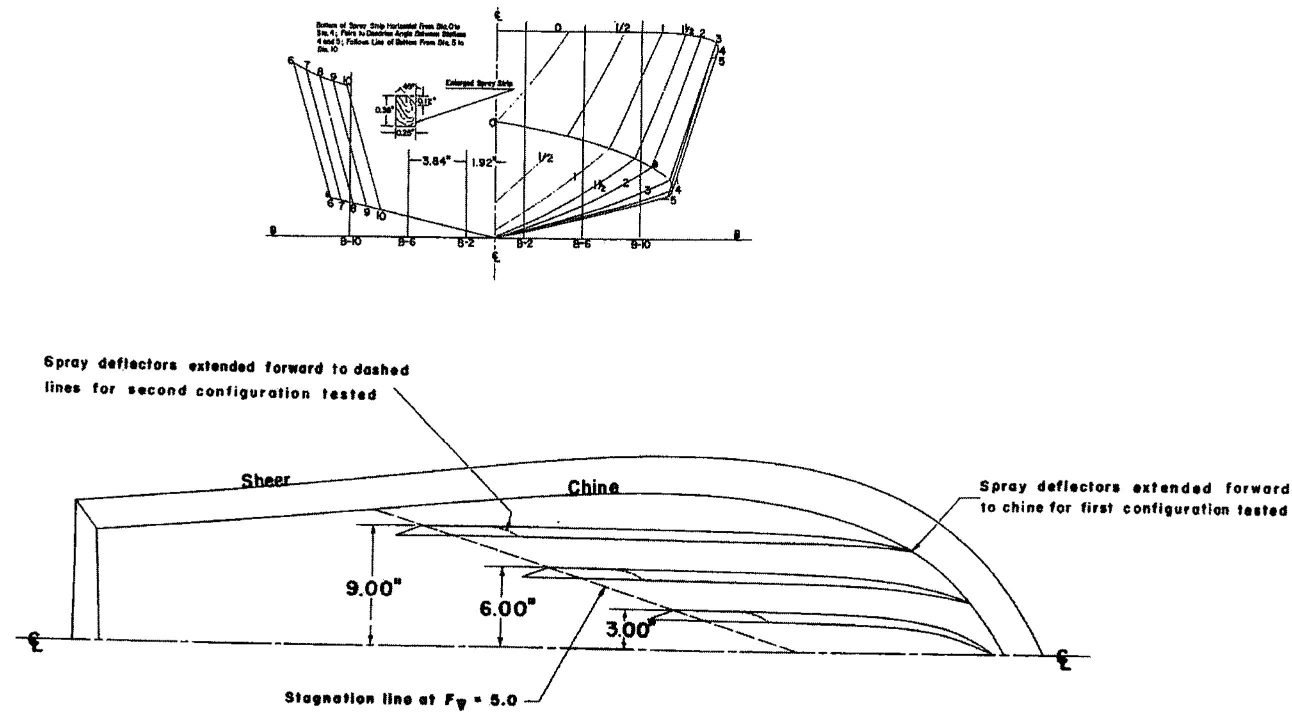

Fig. 10 Hull body plan and spray strips used in model tests of Clement (1964b)

contains a body plan of the specific hull, the principal full-scale geometric dimensions, test displacement, LCG, shaft angle, roughness allowance, frontal area of the hull above the keel, dimensions of skeg (if one was used), and the scale of the test model. The full-scale total resistance versus full-scale speed is plotted on the lower part of each table.

4.3.3. Computational results. Tables 3 to 6 also contain the calculated values of full-scale resistance versus speed. For each hull, the following calculated components of resistance are tabulated separately:

1. Bare hull resistance versus speed
2. Aerodynamic resistance versus speed
3. Whisker spray resistance versus speed
4. Total resistance versus speed.

The methods for calculating each of these resistance components are defined in Tables 3 to 6.

Items 1 and 4 are plotted on the lower part of each table for comparison with the model test results. Of particular interest, these plots also define the speed below which the calculated wetted keel length is estimated to be greater than or approximately equal to 0.90 LWL, thus precluding the use of the computational method for bare hull resistance for this speed range.

4.3.4. Comparison of computed versus experimental results. It is seen that for all test hulls, the differences between calculated total resistance and the results from model tests are less than 5%. This is indeed encouraging, since the calculated total resistance is composed of the sum of three separately computed components.

Further, as previously shown, the agreement between the calculated whisker spray resistance and that measured directly by Clement (1964a, 1964b), and the test results of Kapryan and Boyd (1953) provide additional credibility to the analytical method proposed in this report. The authors encourage additional research of this subject particularly as regards the viscous friction coefficient of the thin sheet of water that constitutes the whisker spray. It has been assumed that in model tests there is a mixture of laminar and turbulent flow in the spray boundary layer and a transitional friction coefficient is required to quantify the friction coefficient as a function of whisker spray Reynolds number. It is believed that further experimental and analytical studies are necessary to understand this flow regime and to develop appropriate viscous coefficients that will be applicable for both model and full-scale Reynolds numbers.

4.3.5. Discussion of results. The data in Tables 3 to 6 illustrate the relative importance of the contribution of whisker spray to the total resistance of a high-speed planing hull. Using the hull shown in Table 4 as an example, the following observations are summarized:

1. The whisker spray resistance increased approximately as the 4.3 power of the speed and was nearly 12% of the bare hull resistance at a maximum speed of 46 knots. This is due mainly to the fact that the trim angle decreases from 9.2 deg at 20 knots to 3.53 deg at 46 knots. Based on the earlier discussions, the lower trim angle orients the spray velocity to a more aft direction so the longitudinal component of its resultant viscous force is increased, thus increasing the hull resistance. The quantity, $\Delta\lambda$, which is a direct indicator of the importance of spray resistance, is seen to increase from a value of 0.06 at 20 knots to a value of 0.42 at 46 knots. This results in a seven-fold increase in resistance due just to a decrease in trim angle. When the quadratic effect of speed is included, the spray drag at 46 knots will be 37 times greater than at 20 knots.

Since high-speed planing hulls are expected to have high deadrise and will naturally run at relatively low trim angles, Fig. 5 shows that the quantity $\Delta\lambda$ will attain large values and hence these hulls are expected to have large spray-induced resistance components. Thus, it is imperative that these hulls be fitted with spray deflectors mounted on the bottom. Recommendations

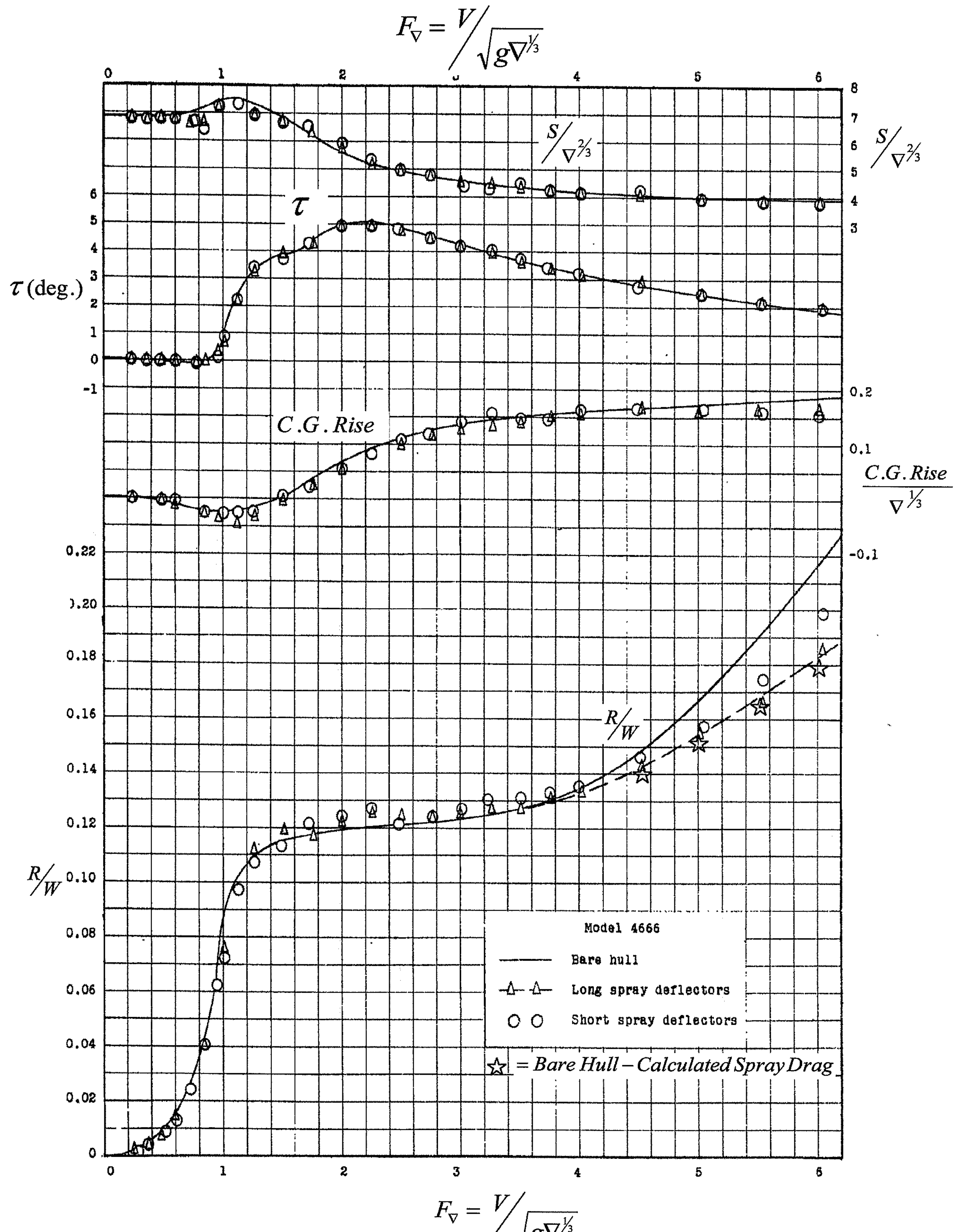

Fig. 11 Effects of two configurations of spray deflectors on the smooth water performance of a planing boat (from Clement 1964b) and compared with spray drag calculated in present study

Table 2 Values of whisker spray drag (88% of calculated maximum spray area wetted)

$F\nabla$	τ	$\Delta\lambda$	2α	Lws	RN†	Cf†	Rs*	Rs/Δ*
4.5	2.9 deg	0.31	39.4 deg	0.76 ft	1.6×10^6	0.0013	940 lbs	0.010
5.0	2.6	0.35	35.6	0.82	1.9×10^6	0.0016	1,630	0.015
5.5	2.2	0.43	30.4	0.95	2.5×10^6	0.0019	2,860	0.028
6.0	2.0	0.48	27.8	1.03	3.0×10^6	0.0021	4,190	0.041

* = full-scale values.
† = model values.

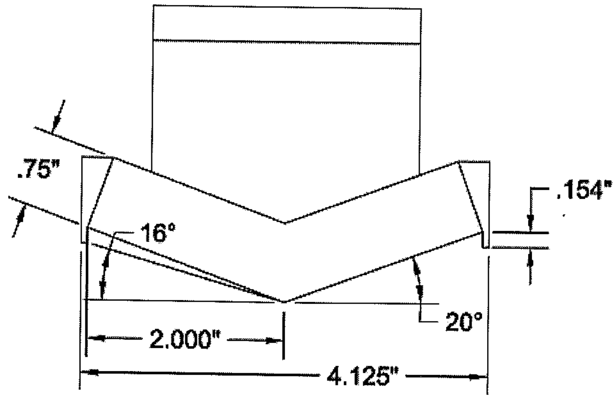

Fig. 12 Sketch and cross section of Langley model 276B

for proper location and design of these deflectors are discussed further in the following section of this paper.

2. The aerodynamic resistance of the bare hull at 46 knots is nearly 6% of the tabulated bare hull resistance. When combined with the whisker spray resistance, their sum will increase the bare hull resistance by nearly 18%. Hence, when using the computational method of Savitsky (1964), it is essential that at high speed the whisker-spray and aerodynamic resistances be added to the results of that computation.
3. The computational method of this paper will allow similar evaluations to be made for other hulls given their geometry, loading, and speed. In some cases it may be that while there is visual evidence of whisker spray emanating from the chines, the combination of running trim and hull deadrise will be such as to direct the spray perpendicular to the keel so that $\Delta\lambda = 0$ and there is no spray contribution to hull resistance.

In summary, these studies indicate that the suggested approach to estimating the whisker-spray resistance appears to be viable. While there is reasonable agreement between the calculated and inferred values of spray resistance (based on three separate series of model tests), the suggested values of model viscous drag coefficient, Cf, in the transition area of the whisker spray must still be verified. It is recommended that additional studies, both experimental and analytical, be made to further quantify Cf in the whisker spray area.

5. Location and design of whisker spray deflectors

5.1. Location and area of whisker spray

The boundaries of the whisker spray flow along the bottom are readily defined by applying the results of calculations such as presented in Tables 3 to 6. Specifically, again using the hull in Table 4 as an example, the following procedure is suggested:

1. The bare hull resistance calculations (item 1) provide the running wetted keel length, Lk, and wetted chine length, Lc, as a function of speed. The line connecting Lk and Lc along the bottom defines the aft boundary of the whisker spray and makes an angle, α, with the keel measured in a plane perpendicular to the hull longitudinal centerplane. This is illustrated in Fig.1.
2. The whisker spray resistance calculations (item 3) define the angle $\theta = 2\alpha$. This is the angle between the forward edge of the spray and the keel, measured in a plane perpendicular to the hull longitudinal centerplane. This is also illustrated in Fig. 1.
3. The bottom area wetted by the whisker spray is thus that bounded by the forward and aft edges of the spray and the chines, as shown by the shaded area in Fig. 1.

5.2. Placement and size of spray deflectors

Clement (1964a, 1964b) demonstrated that three relatively short, longitudinally staggered deflectors whose aft ends are just aft of the stagnation line and are mounted on each side of the bottom will effectively deflect approximately 88% of the spray away from the bottom. As shown in Fig. 8, the transverse locations of the spray strips are approximately ¼, ½, and ¾ of the half beam outboard of the keel. The longitudinal location is such that the aft ends of each strip extend somewhat aft of the stagnation line at each transverse location of the strips. Since the spray location and orientation are functions of speed and loading, the designer should decide the most favorable location of the deflectors to accommodate the high-speed range of operation. Calculated results such as those given in Tables 3 to 6 will provide the necessary guidance for locating and sizing the spray deflectors.

The results of Clement and the present study clearly demonstrate that spray deflectors should be relatively short. If they are so long that they extend aft into the pressure area where the fluid flow is essentially in a longitudinal direction, this extra length will have no effect on the spray but will only add to the total resistance of the hull.

5.3. Cross-section shape of spray deflectors

Muller-Graf (1991) presents the results of an extensive series of model tests to develop a so-called "advanced spray rail system" for semidisplacement hulls. Of particular interest to the planing hull community is the suggested triangular cross-sectional shape of the deflector, as shown in Fig. 14. The sharp outer edge is necessary to facilitate the separation of spray from the hull. Other features are:

ζ = break-off angle of spray deflector >90 deg
δ = bottom angle of spray deflector ≅ 8 deg
b_{sr} = width of spray deflector ≅ 0.005 LWL.

Of course, other naval architects may have different preferences for spray deflector geometries that are based on their own experiences with planing hulls. These hulls are usually shorter than the semidisplacement hulls studied by Muller-Graf.

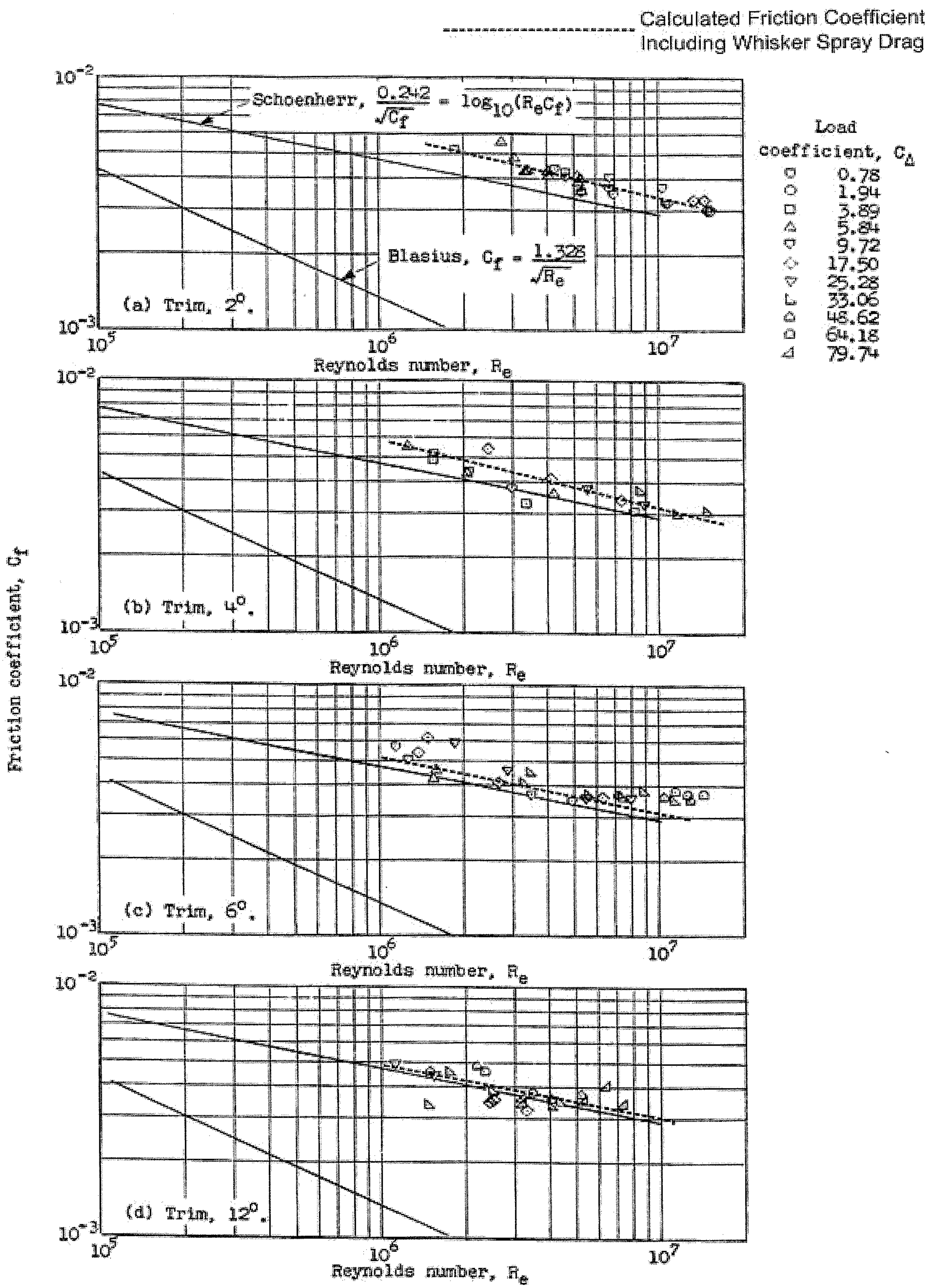

Fig. 13 Friction drag coefficient versus Reynolds number for test model shown in Fig. 12 (from Kapryan & Boyd 1953)

Table 3 **Computed versus measured total resistance**

(Model scale = 12)

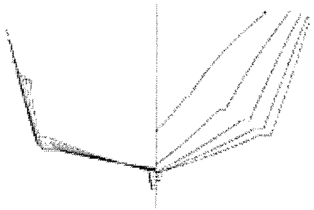

Geometry and test conditions (full-scale values)

Δ = 115,000 pounds
LCG = 28.4 ft forward of transom
Beam @ LCG = 18.2 ft
Deadrise @ LCG = 14 deg
Shaft angle = 12 deg
Frontal area of hull above keel = 216 ft^2
LOA = 81.5 ft
Roughness allowance = 0.0004
Skeg @ keel: L = 36 ft: Area = 65 ft^2: Thickness = 0.40 ft

(1) Bare hull resistance (use method described in Savitsky 1964) + skeg resistance

Vk	*V* (feet/second)	τ (deg)	*Lk* (feet)	*Lc* (feet)	*R*BARE HULL + SKEG (pounds)
28	47.3	3.94	63.0	42.0	13,060
34	57.4	3.84	60.9	39.9	14,590
38	64.1	3.59	58.1	36.2	15,410
42	70.9	3.30	56.8	33.3	16,310
44	74.3	3.16	56.4	30.8	16,820

(2) Aerodynamic resistance = *Ra* (use equation 20)

Vk	28	34	38	42	44
Ra (pounds)	400	580	730	890	980

ρ_{Air} = 0.00234 slugs/ft^3.

(3) Whisker spray resistance (use equation 13 and associated example)

Vk	τ (deg)	$\Delta\lambda$	2α (deg)	*Lws*† (feet)	*RNws*†	*Cf*†	*Rws** (pounds)
28	3.9	0.27	43.4	0.57	7.23E+05	0.0016	300
34	3.8	0.28	42.4	0.58	8.95E+05	0.0014	410
38	3.6	0.30	39.9	0.61	1.05E+06	0.0013	520
42	3.3	0.34	36.9	0.65	1.24E+06	0.0012	650
44	3.2	0.36	35.4	0.68	1.35E+06	0.0011	720

* = full scale.
† = model scale.
v = 0.00001078 ft^2/sec (model tests).

(4) Total resistance *Rt* = *R*BARE HULL + SKEG + *Ra* + *Rws*

Vk	28	34	38	42	44
Rt (pounds)	13,760	15,580	16,660	17,850	18,520

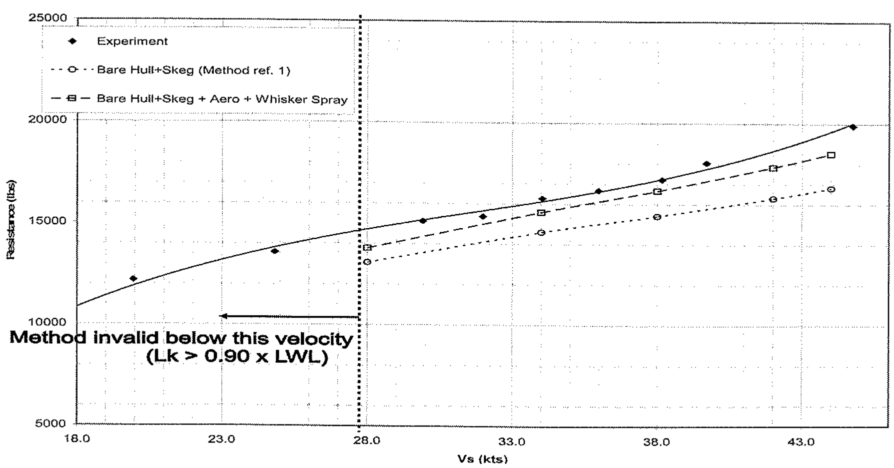

Table 4 Computed versus experimental total resistance

(Model scale = 8)	Geometry and test conditions (full-scale values)
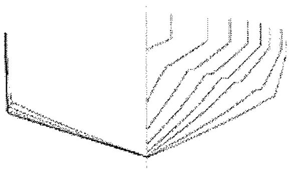	Δ = 38,750 pounds LCG = 13.13 ft forward of transom Beam @ LCG = 13.1 ft Deadrise @ LCG = 19 deg Shaft angle = 0.0 deg Frontal area of hull above keel = 65 ft^2 LOA = 41 ft Roughness allowance = 0.0004

(1) Bare hull resistance (use method described in Savitsky 1964)

Vk	*V* (feet/second)	τ (deg)	*Lk* (feet)	*Lc* (feet)	*R*BARE HULL (pounds)
20	33.8	9.2	25.1	16.3	6,970
25	42.2	7.53	24.9	14.0	6,270
30	50.6	6.12	25.5	12.1	5,810
35	59.1	5.05	26.6	10.4	5,630
40	67.5	4.25	28.0	8.6	5,710
46	77.6	3.53	29.8	6.5	6,070

(2) Aerodynamic resistance = *Ra* (use equation 20)

Vk	20	25	30	35	40	46
Ra (pounds)	60	90	140	190	240	320

ρ_{Air} = 0.00234 slugs/ft^3.

(3) Whisker spray resistance (use equation 13 and associated example)

Vk	τ (deg)	$\Delta\lambda$	2α (deg)	*Lws*† (feet)	*RNws*†	*Cf*†	*Rws** (pounds)
20	9.2	0.06	72.9	0.45	5.01E+05	0.0019	20
25	7.5	0.12	62.2	0.49	6.77E+05	0.0016	60
30	6.1	0.19	52.1	0.55	9.10E+05	0.0014	110
35	5.1	0.26	43.9	0.62	1.21E+06	0.0012	180
40	4.3	0.33	37.5	0.71	1.58E+06	0.0012	310
46	3.5	0.42	31.4	0.83	2.11E+06	0.0017	740

* = full scale.
† = model scale.
v = 0.00001078 ft^2/sec (model tests).

(4) Total resistance *Rt* = *R*BARE HULL + *Ra* + *Rws*

Vk	20	25	30	35	40	46
Rt (pounds)	7,050	6,420	6,060	6,000	6,260	7,130

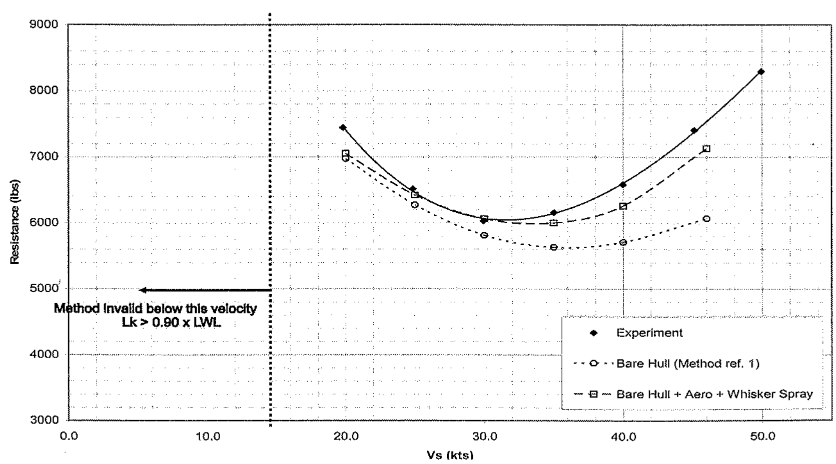

Table 5 Computed versus experimental total resistance

(Model scale = 16)

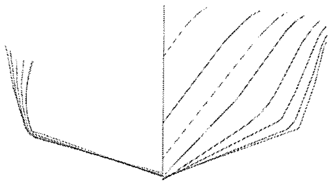

Geometry and test conditions (full-scale values)

Δ = 95,000 pounds
LCG = 27.3 ft forward of transom
Beam @ LCG = 16 ft
Deadrise @ LCG = 19 deg
Shaft angle = 14.4 deg
Frontal area of hull above keel = 150 ft^2
LOA = 69.3 ft
Roughness allowance = 0.0000

(1) Bare hull resistance (use method described in Savitsky 1964)

Vk	*V* (feet/second)	τ (deg)	*Lk* (feet)	*Lc* (feet)	*R*BARE HULL (pounds)
30	50.7	4.09	61.4	36.9	10,570
32	54.1	4.06	59.7	35.0	10,890
34	57.5	3.99	58.5	33.3	11,160
36	60.8	3.89	57.6	31.8	11,410

(2) Aerodynamic resistance = *Ra* (use equation 20)

Vk	30	32	34	36
Ra (pounds)	320	360	400	450

ρ_{Air} = 0.00234 slugs/ft^3.

(3) Whisker spray resistance (use equation 13 and associated example)

Vk	τ (deg)	$\Delta\lambda$	2α (deg)	*Lws*† (feet)	*RNws*†	*Cf*†	*Rws** (pounds)
30	4.1	0.36	36.1	0.45	5.27E+05	0.0018	410
32	4.1	0.37	35.9	0.45	5.65E+05	0.0018	450
34	4.0	0.37	35.3	0.46	6.09E+05	0.0017	510
36	3.9	0.39	34.5	0.47	6.58E+05	0.0016	560

* = full scale.
† = model scale.
v = 0.00001078 ft^2/sec (model tests).

(4) Total resistance *Rt* = *R*BARE HULL + *Ra* + *Rws*

Vk	30	32	34	36
Rt (pounds)	11,300	11,700	12,070	12,420

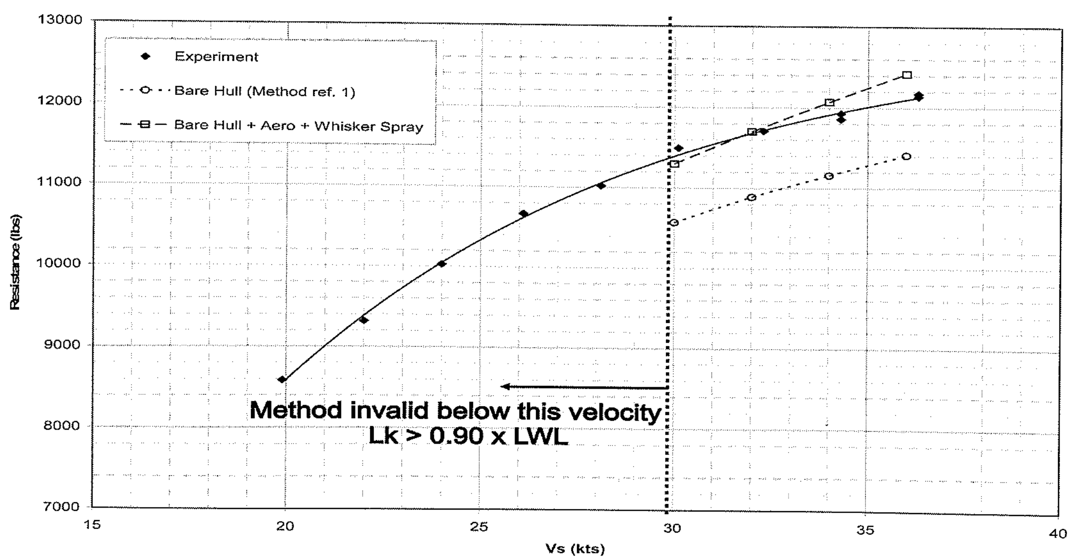

Table 6 Computed versus experimental total resistance

(Model scale = 12)

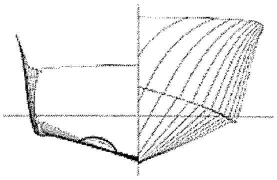

Geometry and test conditions (full-scale values)

Δ = 115,000 pounds
LCG = 27.5 ft forward of transom
Beam @ LCG = 16.2 ft
Deadrise @ LCG = 18.5 deg
Shaft angle = 10 deg
Frontal area of hull above keel = 164 ft^2
LOA = 74.5 ft
Roughness allowance = 0.0004

(1) Bare hull resistance (use method described in Savitsky 1964)

Vk	*V* (feet/second)	τ (deg)	*Lk* (feet)	*Lc* (feet)	$R_{\text{BARE HULL}}$ (pounds)
30	50.6	4.82	58.6	38.2	14,230
32	54.0	4.77	57.0	36.4	14,580
34	57.4	4.67	55.8	34.8	14,860
36	60.8	4.54	55.0	33.3	15,120
38	64.1	4.39	54.4	32.0	15,360
40	67.5	4.22	54.0	30.7	15,620

(2) Aerodynamic resistance = *Ra* (use equation 20)

Vk	30	32	34	36	38	40
Ra (pounds)	340	390	440	500	550	610

ρ_{Air} = 0.00234 slugs/ft^3.

(3) Whisker spray resistance (use equation 13 and associated example)

Vk	τ (deg)	Δλ	2α (deg)	*Lws*† (feet)	*RNws*†	*Cf*†	*Rws** (pounds)
30	4.8	0.27	43.2	0.52	7.03E+05	0.0016	280
32	4.8	0.27	42.8	0.52	7.56E+05	0.0015	310
34	4.7	0.28	42.0	0.53	8.15E+05	0.0015	350
36	4.5	0.29	40.9	0.54	8.82E+05	0.0014	390
38	4.4	0.31	39.6	0.56	9.55E+05	0.0014	430
40	4.2	0.33	38.2	0.57	1.04E+06	0.0013	490

* = full scale.
† = model scale.
v = 0.00001078 ft^2/sec (model tests).

(4) Total resistance *Rt* = $R_{\text{BARE HULL}}$ + *Ra* + *Rws*

Vk	30	32	34	36	38	40
Rt (pounds)	14,850	15,280	15,650	16,010	16,340	16,720

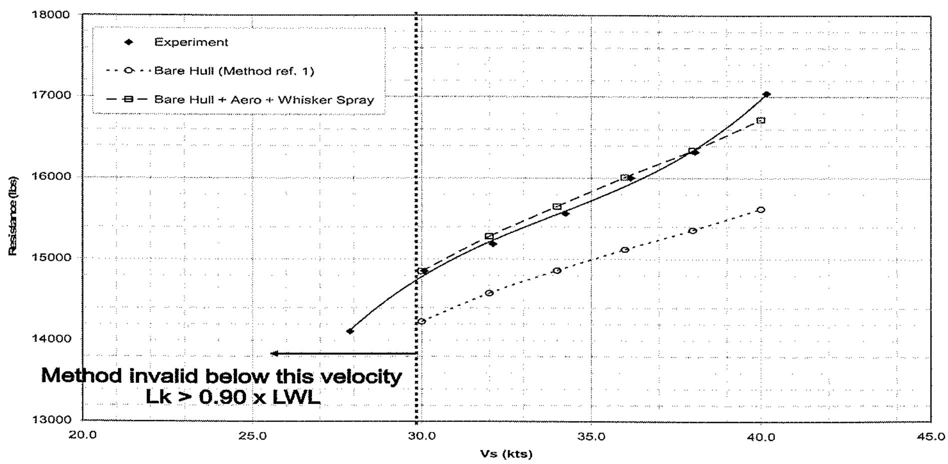

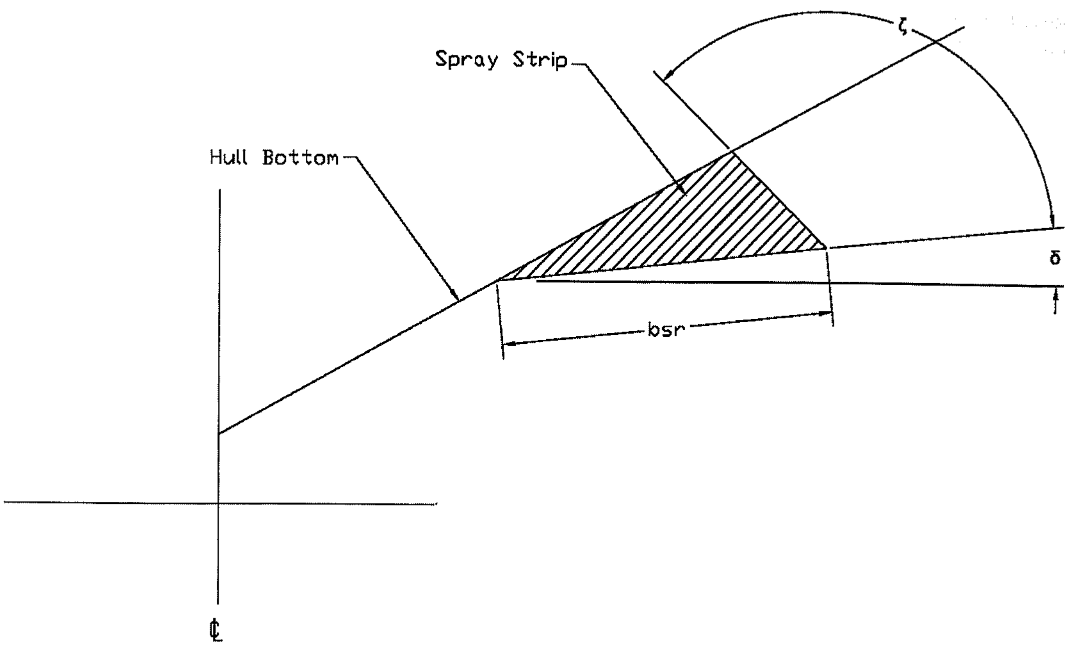

Fig. 14 Suggested spray rail geometry

The recommended sharpness of the outer edge of the deflector cannot be overemphasized. Even a slight rounding of this edge may cause the flow to remain attached to the deflector and thus reduce its ability to deflect the spray sheet; Clement (1964a) shows that a rounded edge (approximately ¼ in., full scale) nearly negated the effectiveness of the deflector. This may present a problem for hulls that are constructed in molds where the spray deflectors are an integral part of the bottom and thus may be difficult to manufacture with a sharp outer edge.

6. Relation between calculated and measured trim angle

The computational method of Savitsky (1964) is based on the hydrodynamics of prismatic surfaces where the buttock lines are straight and parallel. Thus, the calculated trim angle, relative to the level water surface, is the same for every buttock line. This angle is referred to as the "hydrodynamic" trim angle.

The reference for the trim angle recorded by towing tanks during tests of conventional warped (nonprismatic) hulls may vary according to the preferences of the test facility or the designer. For example, the trim angle may be the angle between the keel and the level water line, the angle between the lower edge of the skeg and the level water line, the angle of the design water line relative to the level waterline, and so forth. Consequently, a direct comparison of the calculated trim with the trim angle reported by the towing tank may not be meaningful.

A brief attempt was made to correlate the computed trim angle with the geometry of the tested nonprismatic hulls. Some of the tested hulls had a small amount of warp (deadrise increasing with increasing distance forward of the transom) so that some of the buttock lines were at a positive trim angle relative to the level water surface even in the static condition. Other hulls had a shallow transom draft so that the aft length of the keel was at a negative trim relative to the level water line in the static condition. Consequently, when planing, the angle of attack (relative to the level water surface) at any point on the bottom varies according to its longitudinal and transverse location. It would be useful to establish both an effective trim and deadrise for warped surfaces. This will require additional systematic model tests supported by analytical studies. Unfortunately, presently there is no apparent sponsor for such a study.

In the interim, the present limited study suggests that the effective deadrise and beam for a warped surface can be taken as that at the LCG. Relative to the effective trim angle, the results of this study suggest that the effective trim can be taken as the geometric trim angle (relative to the level water surface) of the 1/4 buttock line measured at the forward edge of the stagnation line.

7. Conclusions

An analytical procedure is developed for calculating the resistance of the leading edge whisker spray associated with planing craft. It is shown that the magnitude of this resistance component is dependent on the running trim and hull deadrise. It is largest for high deadrise hulls operating at relatively low trim angles, a combination that is typical for very high-speed hulls. In fact, the whisker spray resistance can be as large as 15% of the bare hull resistance and must be included when estimating the total resistance of high-speed hulls. The present report applies the computation method to estimate the total resistance of four arbitrarily selected planing hulls that were model tested at the Davidson Laboratory and shows rather good agreement with experimental data.

It is shown that the whisker spray can be deflected from the hull bottom (with a consequent reduction in hull resistance) by installing relative short longitudinal spray strips mounted on the bottom. Guidance is provided for the proper location, size, and geometric shape of these strips.

In model tests, the whisker spray flow along the bottom is shown to be in a transitional state between laminar and turbulent flows. An equation for its friction coefficient as a function of local Reynolds number is developed. However, it is recommended that additional experimental and analytical studies be undertaken to further define the viscous drag coefficient for model and full-scale planing craft.

Acknowledgments

The authors are indebted to the T&R Steering Committee of the Society of Naval Architects and Marine Engineers for their encouragement to undertake this study and for providing partial financial support for it. They also thank Mr. Joseph G. Koelbel, Jr., naval architect, for his thorough review of the paper.

References

CLEMENT, E. P. 1964a *Effects of Longitudinal Bottom Spray Strips on Planing Boat Resistance*, David Taylor Model Basin, Department of the Navy, Report No. 1818, February.

CLEMENT, E. P. 1964b *Reduction of Planing Boat Resistance by Deflection of the Whisker Spray*, David Taylor Model Basin, Department of the Navy, Report No. 1929, November.

CLEMENT, E. P., AND BLOUNT, D. L. 1963 Resistance tests of a systematic series of planing hull forms, *Transactions of the Society of Naval Architects and Marine Engineers*, **71**.

KAPRYAN, W. J., AND BOYD, JR., G. M. 1953 *The Effect of Vertical Chine Strips on the Planing Characteristics of V-Shaped Prismatic Surfaces Having Angles of Deadrise of 20 deg. and 40 deg.*, NACA Technical Note 3052, November.

MULLER-GRAF, B. 1991 The effect of an advanced spray rail system on resistance and development of spray of semi-displacement round bilge hulls, *Proceedings*, FAST '91, June, Trondheim, Norway.

SAVITSKY, D. 1964 Hydrodynamic design of planing hulls, MARINE TECHNOLOGY, **1**, 1.

SAVITSKY, D., AND BRESLIN, J. P. 1958 *On the Main Spray Generated by Planing Surfaces*, Davidson Laboratory, Stevens Institute of Technology, Hoboken, NJ, Report No. 678, January.

SAVITSKY, D., AND NEIDINGER, J. W. 1954 *Wetted Area and Center of Pressure of Planing Surfaces at Very Low Speed Coefficients*, Davidson Laboratory, Stevens Institute of Technology, Hoboken, NJ, Report No. 493, July.

SAVITSKY, D., AND ROSS, E. W. 1952 *Turbulence Stimulation in the Boundary Layer of Planing Surfaces-Part II*, Davidson Laboratory, Stevens Institute of Technology, Hoboken, NJ, Report No. 444, August.

SCHLICHTING, H. 1960 *Boundary Layer Theory*, 4th ed., McGraw-Hill, New York.

SCHOENERR. 1932 Resistance of flat surfaces moving through a fluid, *Transactions of the Society of Naval Architects and Marine Engineers*, **40**.

SNAME. 1948 *Uniform Procedure for the Calculation of Frictional Resistance and the Expansion of Model Data to Full Size*, Bulletin No. 1–2, Society of Naval Architects and Marine Engineers, Jersey City, NJ.

WEINSTEIN, I., AND KAPRYAN, W. J. 1953 *The High-Speed Planing Characteristics of a Rectangular Flat Plate Over a Wide Range of Trim Angle and Wetted Length*, NACA Technical Report No. 2981, July.

Appendix 1

Aerodynamic resistance of planing hull models

The performance prediction method in Savitsky (1964) does not include the aerodynamic drag of the hull cross-sectional area above the waterline. This is of importance during model tests where the design naval architect may be comparing tank data (using a hull model without superstructure) with computer estimates. Because this aerodynamic drag increases as the square of the towing speed, it becomes a significant component of the total resistance at maximum speed.

In order to quantify this drag component, the Davidson Laboratory measured the drag of many models of planing monohulls towed over a wide speed range with the hulls set at a trim angle of 0 deg and raised just above the level waterline. (There was no hull wetting.) It was found that for typical bow plan forms, the drag coefficient, based on the frontal area of the hull, was approximately equal to 0.70.

Thus, the aerodynamic drag of the hull can be estimated by the following simple equation:

$$R_{\text{Air}} = \frac{1}{2}\,\rho_{\text{Air}}\,V^2\,Ah \times Cd \qquad \text{(A1)}$$

where

R_{Air} = aerodynamic resistance of hull

V = velocity, (towing speed ± wind speed) (feet/second)

Ah = frontal area of hull (square feet)

ρ_{Air} = air density (lb–sec^2/ft^4)

Cd = aerodynamic drag coefficient based on frontal area of the hull = 0.70

Of course, the naval architect will include both the hull frontal area and the above deck structure when estimating the total aerodynamic resistance of the craft. These resistance components must be included when estimating the powering requirements of planing craft at high speed.